Microwave properties of borocarbide superconductors RNi$_2$B$_2$C (R=Y,Er,Tm,Ho)

T. Jacobs, Balam A. Willemsen, and S. Sridhar

Physics Department, Northeastern University, Boston, Massachusetts 02115

R. Nagarajan, L. C. Gupta, Z. Hossain, and Chandan Mazumdar

Tata Institute of Fundamental Research, Colaba, Bombay, India

P. C. Canfield and B. K. Cho

Ames Laboratory and Department of Physics and Astronomy, Iowa State University, Ames, Iowa

We report measurements of the microwave surface impedance of the borocarbide family of superconductors RNi$_2$B$_2$C (R=Y,Er,Tm,Ho). The experiments enable direct measurements of the superfluid density, and are particularly sensitive to the influence of magnetic pair breaking. In HoNi$_2$B$_2$C the antiferromagnetic transition is clearly observed at zero field, and leads to a drastic reduction of the superfluid density, which recovers at lower temperatures. In ErNi$_2$B$_2$C the antiferromagnetic transition is not seen in zero-field data. Magnetic effects are responsible for anomalies in the low-temperature surface impedance below approximately 4 K in HoNi$_2$B$_2$C and TmNi$_2$B$_2$C. The temperature dependence of the microwave impedance disagrees with BCS calculations.

Recently superconductivity was discovered in quaternary multiphase Y-Ni-B-C,[1] in multiphase Y-Pd-B-C system,[2] and in single-phase RNi$_2$B$_2$C (R=Y,Ho,Er,Tm,Lu).[3] These materials are a class of intermetallic superconductors. While some members of the family, e.g., YNi$_2$B$_2$C, appear to show conventional superconducting behavior,[4,5] other members, with R=Tm,Er,Ho, undergo an antiferromagnetic (AFM) transition at T_N, below the superconducting transition at T_c. Thus in addition to the important question of the nature of superconductivity issues concerning the interplay of magnetism and superconductivity arise in these materials.

Microwave measurements of superconductors yield unique information regarding the superfluid density, the quasiparticles, and the nature of the pairing.[6] Despite the fact that magnetic superconductors such as ErRhB$_4$ have been known for about two decades, there have been few microwave studies of such superconductors. In this paper we report measurements of the microwave response of several members of the family, RNi$_2$B$_2$C with R=Y,Er,Tm,Ho.

Single crystals of RNi$_2$B$_2$C were grown out of Ni$_2$B flux. Details are provided in Ref. 5. The crystals have a platelike morphology and x-ray diffraction indicates that they have their crystallographic c axis perpendicular to the surface of the plate. Powder x-ray diffraction on ground single crystals indicates that there is a small amount of Ni$_2$B flux contaminating the crystal, probably on the surface. This contamination is estimated to be below the 5% level. These crystals have been extensively characterized by a variety of techniques[5,7–9] besides the microwave studies discussed here. Polycrystalline samples of YNi$_2$B$_2$C were also prepared and measured.

Microwave measurements were carried out in a Nb cavity using a high-precision "hot finger" method,[10] in which the cavity is maintained at 2 K while the sample temperature is varied from 2 K to as high as 200 K. The surface resistance of the sample is obtained from measurements of the resona-

tor Q using $R_s = \Gamma [Q_s^{-1}(T) - Q_0^{-1}(T)]$, where Q_s and Q_0 are, respectively, the resonator Q's with and without the sample. Similarly changes in the reactance are obtained from $\Delta X_s = \mu_0 \omega \Delta \lambda = (-2\Gamma/f_0) [f_s(T) - f_0(T)]$, where f_s and f_0 represent the resonant frequency with and without the sample. To get the absolute value of the reactance, an indeterminate constant X_0 needs to be added. In materials which obey the skin-depth limit in the normal state, one can use the criterion that $R_n = X_n$ above T_c to determine X_0 and so the absolute value of X_s. The geometric constant Γ was calculated, and confirmed using measurements on known samples of Cu. The method has been extensively validated via measurements on a variety of samples, from conventional low-temperature superconductors, to high-temperature superconducting crystals and films.[11]

Because we are able to measure both the real and imaginary parts of the impedance $Z_s = R_s + iX_s$, it is possible to obtain the complex conductivity $\sigma_s = \sigma_1 - i\sigma_2$ from the present measurements, using the relation $Z_s = R_n \sqrt{2i/(\sigma_s/\sigma_n)}$, where R_n and σ_n are the normal-state surface resistance and conductivity, respectively. Of particular importance is the imaginary part σ_2. This quantity is a measure of the superfluid density n_s which is proportional to σ_2. It is also related to the penetration depth via $\sigma_2 = 1/\mu_0 \omega \lambda^2$.

The microwave resistivity $\rho_{\mu n}(T)$ in the normal state, see Fig. 1, was obtained from the surface resistance using $R_n = \sqrt{\pi \mu_0 f \rho_{\mu n}}$ where μ_0 is the permeability of free space. The data are in good agreement with dc measurements,[12] confirming that the classical skin-depth regime applies in the normal state.

YNi$_2$B$_2$C

The superconducting surface resistance $R_s(T)$ of several samples of YNi$_2$B$_2$C are shown in Fig. 2. The polycrystal

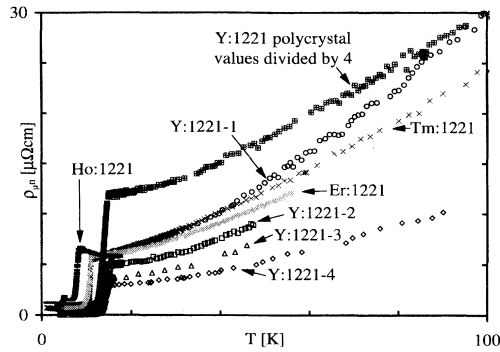MICROWAVE PROPERTIES OF BOROCARBIDE...

FIG. 1. Microwave resistivity of RNi_2B_2 (R=Y,Er,Tm,Ho) in the normal and superconducting states extracted from the surface resistance.

shows higher R_n and also a slightly broader transition than single crystals. It is evident that R_s does not go to zero as $T \rightarrow 0$. There is a residual surface resistance which is of the order of 10–20 mΩ and is, possibly, extrinsic in origin. This residual resistance does depend on sample characteristics such as crystallinity and surface preparation, being lowest for the polished single-crystal Y:1221-4. This is probably due to slight flux contamination which leads to a temperature-independent microwave loss.

Figure 2 also shows the surface reactance $X_s(T)$. The absolute value was obtained by normalizing to $X_n = R_n$ above T_c. A striking feature of the reactance X_s data is the peak near T_c. This can be understood from simple models of the superconducting state such as two fluid or BCS. This is in fact occasionally observed in other superconductors, and is due to buildup of superfluid, which leads to a situation where $\lambda > \delta_n$, the superconducting penetration depth is bigger than the normal-state skin depth. This results in a peak in X_s which we have observed in $YBa_2Cu_3O_{1-\delta}$ also.[13] If we substract the residual resistance from the low-temperature reactance we can estimate a zero-temperature penetration depth $\lambda(0) = 1100$ Å for sample Y:1221-1. Although this method is not very sensitive to the absolute magnitudes the agreement with other estimates of $\lambda(0) = 1200$ Å is good.[5]

$TmNi_2B_2C$

While the overall behavior of $TmNi_2B_2C$ near and slightly below T_c is similar to the Y compound (see Fig. 3),

FIG. 3. R_s and X_s of $TmNi_2B_2C$ and $ErNi_2B_2C$.

a noteworthy feature is the *increase* of R_s at low temperatures. This is due to increasing magnetic coherence which results in an AFM transition at 1.5 K,[14] which is, however, just below the lower limit of our apparatus. This is also consistent with a decrease of H_{c2} observed in the same temperature region.[15] The data demonstrate that the microwave measurements can provide a measure of the magnetic scattering through the influence on the surface impedance of the superconducting state.

$ErNi_2B_2C$

The response of this compound appears similar to that of the Y compound as shown in Fig. 3. Interestingly the AFM transition which should occur at 6.0 K (Refs. 16 and 15) as observed in specific-heat, dc-resistivity, and magnetic-susceptibility measurements, does not appear in the microwave data. Thus in this compound, the AFM transition is not accompanied by pair breaking in zero field. There is, however, a weak shoulder in the R_s data at around 9.5 K which is not associated with a feature in any other measurement.

$HoNi_2B_2C$

A detailed plot of $R_s(T)$ vs T in the region from 2 to 10 K is shown in Fig. 4. The drop in R_s at the superconducting transition temperature of 8 K is clearly seen. In all conventional superconductors, and in YNi_2B_2C as shown above, R_s decreases monotonically from the normal-state value R_n. Remarkably, in $HoNi_2B_2C$ R_s starts to increase again at
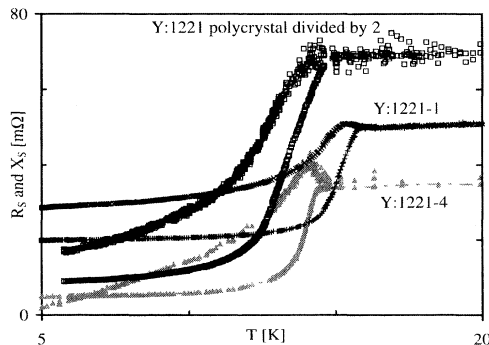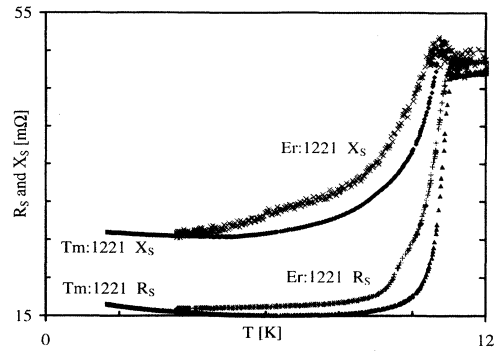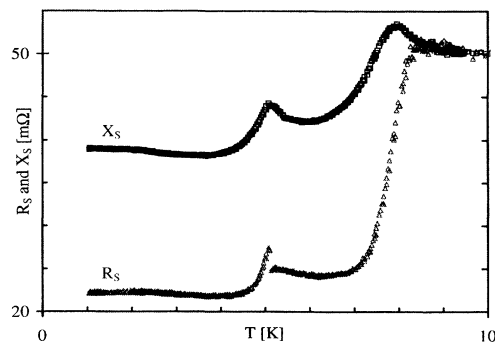

FIG. 2. R_s and X_s of YNi_2B_2C in the superconducting state for a polycrystal and single crystals (Y:1221-1 and Y:1221-4).

FIG. 4. R_s and X_s of $HoNi_2B_2C$. The AFM transition at 5.2 K is clearly visible.
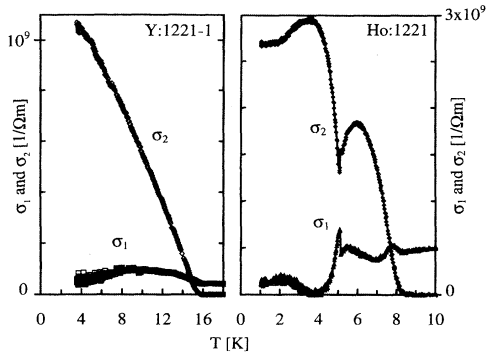
FIG. 5. Real (σ_1) and imaginary (σ_2) parts of the complex conductivity of (left) YNi$_2$B$_2$C and (right) unpolished HoNi$_2$B$_2$C sample. σ_2 is proportional to the superfluid pair density.

around 6 K. This is due to pair breaking which accompanies the development of the antiferromagnetic state. At the AFM transition, R_s shows a *peak*. Peaks in R_s are never seen in conventional superconductors, although nonmonotonic dependence has been observed in YBa$_2$Cu$_3$O$_{1-\delta}$.[17]

It is very interesting to study the reactance as a function of temperature, also shown in Fig. 4. Below the superconducting transition at 8 K, X_s increases due to the buildup of superfluid, as for the other superconductors, and then starts to decrease. However, the AFM transition intervenes and appears as a peak, due to pair breaking.

At low temperatures, both R_s and X_s are seen to *increase with decreasing T*. Although this is similar to that observed in TmNi$_2$B$_2$C, there is no AFM transition at a comparable temperature. Thus our data indicate a possibly new source of magnetic scattering below about 3.75 K.

COMPLEX CONDUCTIVITY AND SUPERFLUID DENSITY

The real and imaginary parts of the conductivity σ_1 and σ_2 of YNi$_2$B$_2$C are shown in Fig. 5. Note that a residual $R_{s, \text{res}}$ was subtracted while computing the complex conductivity. σ_2 has a "conventional" temperature dependence in that it rises smoothly at T_c to a large value at low temperatures. However, the detailed temperature dependence does not fit any conventional form such as $(1-t^4)$ of the two-fluid model or a BCS form. Instead σ_2 appears to be well described by a $(1-t)$ temperature dependence, except for a very slight curvature. The larger coherence length, low measured penetration depth, and the obvious magnetic influence in the other components make it unlikely that the present anomalous behavior can be attributed to weak links, as has been claimed for the copper oxides.[18] σ_1 rises from its normal-state value and has a peak at around $0.5T_c$. This is not the behavior expected from BCS coherence factors since there the peak is around $0.9T_c$. Instead this is similar to the behavior of σ_1 of YBa$_2$Cu$_3$O$_{7-\delta}$ where there is a broad peak at around $0.4T_c$.[17]

In HoNi$_2$B$_2$C, σ_2 and hence n_s are found to initially increase (see Fig. 5). However, the AFM transition arrests this increase, and *reduces the superfluid density*, although superconductivity is not completely destroyed since σ_2 does not become zero. Below the AFM transition, σ_2 recovers. It is interesting that the behavior of σ_2 very closely mirrors that
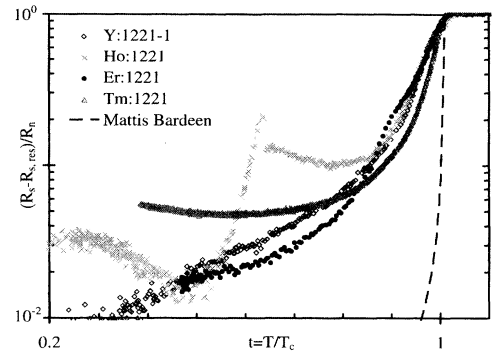

FIG. 6. Normalized surface resistance of RNi$_2$B$_2$C (R = Y,Tm,Er,Ho) in the superconducting states vs reduced temperature. The residual R_s ($T\rightarrow0$) has been subtracted out in each case. Also shown are BCS calculations with $\Delta(0)kT_c$ = 1.74 (dashed line) and 0.45 (solid line).

of H_{c2}.[9] The AFM transition is also reflected in the temperature dependence of σ_1.

DISCUSSION AND COMPARISON WITH THEORY

In order to address the issue of the nature of the superconducting order parameter we plot the normalized surface resistance $[R_s(T) - R_{s, \text{res}}]/R_s(T_c)$ vs $t = T/T_c$ for all the superconductors that were measured. The resulting scaled plot shown in Fig. 6 is noteworthy in that it appears to indicate a common, underlying temperature dependence, independent of sample, except of course for the expected deviations near T_N in HoNi$_2$B$_2$C and the low-temperature rise for HoNi$_2$B$_2$C and TmNi$_2$B$_2$C. For comparison, the normalized surface impedance calculated from a Mattis-Bardeen conductivity in the local limit is also plotted using a gap ratio of $\Delta(0)/kT_c$ = 1.76.

Separate comparisons were also carried out for the YNi$_2$B$_2$C data with isotropic scaled weak-coupling theory.[19] The calculations were done using parameters $\Delta(0)/kT_c$ = 1.76 and $\xi_{\text{GL}}(0)$ between 50 and 120 Å, typical of those found in the literature. A mean free path of 150 Å was chosen to agree with the normal-state resistivity data. The London penetration depth λ_L = 900 Å was adjusted to fit the low-T X_s data. Even this more complete BCS s-wave calculation does not agree with the present data significantly better than simple Mattis-Bardeen. The disagreement appears to be in conflict with other measurements which generally find agreement with BCS behavior.[14,20,21]

The microwave data differ from the BCS analysis in three ways: (1) a broader temperature dependence near T_c in all the superconductors as evident in Fig. 6, (2) the peaks at the AFM transition in HoNi$_2$B$_2$C, and (3) the low-temperature rise in HoNi$_2$B$_2$C and TmNi$_2$B$_2$C. The latter two features can be attributed to pair breaking by the magnetic constituents Ho and Tm. While the first feature could arise from sample inhomogeneities at the surface, an interesting question is whether the broadened transition could be due to an unidentified source of pair breaking which should then be present in all the compounds. Equally noteworthy is the absence of any signature of the AFM transition in the Er superconductor. Neutron-scattering studies of HoNi$_2$B$_2$C (Ref. 7)

have shown the existence of a modulated magnetic structure from 6 to about 4.7 K. Similar features are not observed in $ErNi_2B_2C$.[22,23] Pair breaking is significant only when there exists magnetic fields over length scales comparable to the coherence length, and this appears to occur in $HoNi_2B_2C$, but not in $ErNi_2B_2C$.

In conclusion, the microwave properties of several borocarbide superconductors reveal interesting features of the superconducting state. The superfluid density which is obtained from the data displays striking features due to the influence of magnetic pair breaking. The data reveal interesting results on the interplay of magnetism and superconductivity which deserve further experimental and theoretical studies.

[1] R. Nagarajan et al., Phys. Rev. Lett. **72**, 274 (1994).

[2] R. J. Cava et al., Nature (London) **367**, 146 (1994).

[3] R. J. Cava et al., Nature (London) **367**, 252 (1994).

[4] S. A. Carter et al., Phys. Rev. B **50**, 4216 (1994).

[5] M. Xu et al., Physica C **227**, 321 (1994).

[6] S. Sridhar, D.-H. Wu, and W. L. Kennedy, Phys. Rev. Lett. **63**, 1873 (1989).

[7] A. I. Goldman et al., Phys. Rev. B **50**, 9668 (1994).

[8] L. P. Le et al., Physica B **206**, 552 (1995).

[9] P. C. Canfield et al., Physica C **230**, 397 (1994).

[10] S. Sridhar and W. L. Kennedy, Rev. Sci. Instrum. **59**, 531 (1988).

[11] S. Oxx et al., Physica C **235-240**, 889 (1994).

[12] D. Naugle (private communication).

[13] H. J. Chen, J. Owliaei, and S. Sridhar, Rev. Sci. Instrum. **65**, 2635 (1994).

[14] R. Movshovich et al., Physica C **227**, 381 (1994).

[15] H. Eisaki et al., Phys. Rev. B **50**, 647 (1994).

[16] B. K. Cho, P. C. Canfield, L. L. Miller, D. C. Johnston, W. P. Beyermann, and A. Yatska, Phys. Rev. B **52**, 3684 (1995).

[17] D. A. Bonn, P. Dosanjh, R. Liang, and W. N. Hardy, Phys. Rev. Lett. **68**, 2390 (1992).

[18] J. Halbritter, J. Appl. Phys. **71**, 339 (1992).

[19] J. Halbritter, Z. Phys. **266**, 209 (1974).

[20] T. Ekino et al., Physica C **235-240**, 2529 (1994).

[21] T. Hasegawa et al., Physica C **235-240**, 1859 (1994).

[22] S. K. Sinha et al., Phys. Rev. B **51**, 681 (1995).

[23] J. Zaretsky et al., Phys. Rev. B **51**, 678 (1994).